Copper/photoredox catalysis enables desulfonylative radical *N*-glycosylation

Qikai Sun[1#], Quanquan Wang[2#], Wenzhuo Qin[1], Kaiyu Jiang[1], Gang He[1], Ming Joo Koh[2]* and Gong Chen[1,3,4]*

[1]State Key Laboratory and Institute of Elemento-Organic Chemistry, College of Chemistry, Nankai University, Tianjin 300071, China

[2]Department of Chemistry, National University of Singapore, 4 Science Drive 2, Singapore, 117544, Republic of Singapore

[3]Frontiers Science Center for New Organic Matter, Nankai University, Tianjin 300071, China

[4]Haihe Laboratory of Sustainable Chemical Transformations, Tianjin 300192, China

[#] Q.S. and Q.W. contributed equally to this work.

*Corresponding author emails: chmkmj@nus.edu.sg (M.J.K.), gongchen@nankai.edu.cn (G.C.)

Abstract

The state-of-the-art for glycosylation primarily relies on the classical polar reactions of heteroatomic nucleophiles with electrophilic glycosyl oxocarbenium intermediates. While such an ionic glycosylation strategy has worked well to deliver *O*-glycosides, its utilization in *N*-glycoside synthesis is often plagued by the subdued reactivity of *N*-nucleophiles under the acidic reaction conditions required for activating glycosyl donors. Exploring the reactivity of glycosyl radical intermediates could open up new glycosylation pathways. However, despite the recent significant progress in radical-mediated synthesis of *C*-glycosides, harnessing the reactivity of glycosyl radicals for the generation of canonical *O*- or *N*-glycosides remains elusive. Herein, we report the first examples of glycosyl radical-mediated *N*-glycosylation reaction using readily accessible glycosyl sulfone donors and *N*-nucleophiles under mild copper-catalyzed photoredox-promoted conditions. The method is efficient, selective, redox-neutral, and broadly applicable, enabling facile access to a variety of complex *N*-glycosides and nucleosides in a streamlined fashion. Importantly, the present system tolerates the presence of water and offers unique chemoselectivity, allowing selective reaction of NH sites over hydroxyl groups that would otherwise pose challenges in conventional cationic *N*-glycosylation.

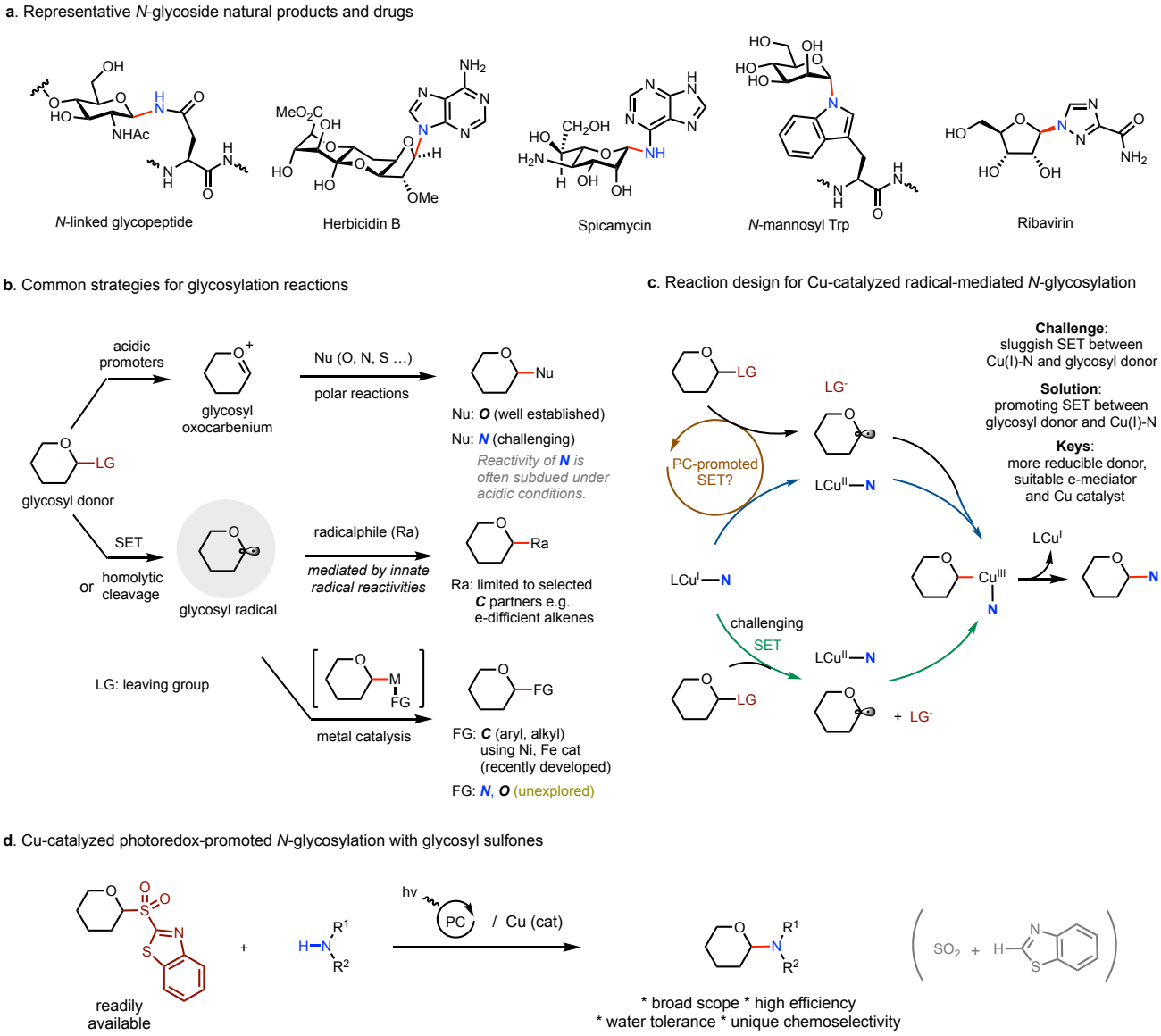

Figure 1. Glycosyl radical-mediated synthesis of *N*-glycosides.

Carbohydrates play a central role in many biological processes and have important applications in modern therapeutic developments[1-3]. *O*- and *N*-glycosides bearing oxygen or nitrogen linkers at the anomeric position, respectively, are the two most prevalent classes of carbohydrates[2, 4, 5]. Compared to divalent oxygen atoms, trivalent nitrogen atoms can adopt more diverse bonding patterns, and their reactivities can be more strongly influenced by steric and electronic factors[6]. The versatile bonding abilities of nitrogen give *N*-glycosides rich structural features that enable their varied biological functions[7, 8]. For example, nucleosides bearing heteroaromatic nitrogen motifs are the key building blocks of nucleic acids, and nucleoside analogs are commonly found in natural products (e.g. Herbicidin)[9] and widely used in drug development (e.g. Ribavirin)[10] (**Figure 1a**). *N*-glycosylation of the carboxamide side chain of glutamine (*N*-glycan) represents an important mode of posttranslational modification of proteins[11]. However, the distinct chemical properties of various nitrogen motifs, especially their basicity, also pose a significant challenge to the synthesis of *N*-glycosides[5].

The existing strategies for constructing the glycosidic bond mostly rely on the polar reactions of heteroatomic nucleophiles with electrophilic glycosyl oxocarbenium intermediates, which are typically generated from glycosyl donors under acidic conditions[5, 7, 12-15]. While the acid-promoted substitution regime works well for most *O*-nucleophiles such as OH groups of alcohols[2, 16, 17], it is not particularly well-suited for more basic *N*-nucleophiles, whose reactivity can be diminished under the reaction conditions[12, 18]. To enhance *N*-glycosylation efficiency, more forcing conditions such as higher temperatures are often required, but this can cause problems with acid-labile functional groups[19]. In addition, oxocarbenium pathways lack the ability to effectively distinguish different types of nucleophiles, resulting in the need for extensive use of protecting groups for intricate substrates and rigorous removal of water from the reaction system[20, 21]. On the other hand, glycosyl radical intermediates have different reactivity patterns compared to oxocarbenium ions[22-24]. Exploration of the glycosyl radical-mediated reactivity could unlock new avenues for constructing glycosidic bonds (**Figure 1b**). Unsurprisingly, the innate reactivity of glycosyl radicals has long been leveraged to make *C*-glycosides by reacting with strong radicalphiles such as electron-deficient alkenes or heteroarenes[25-30]. More recent studies showed that the reactivity of glycosyl radicals could be further modulated by metal catalysts such as nickel and iron complexes to make *C*-glycosides in a more controlled manner[31-34]. However, the corresponding reactions of glycosyl radicals with *N*- or *O*-based reagents for accessing canonical *N*- or *O*-glycosides remain largely elusive[35, 36].

Copper has a unique ability to catalyze the coupling of heteroatoms such as N and O with carbon-based partners[37, 38]. Over the past decade, radical-mediated copper-catalyzed C-N coupling chemistry has provided a powerful platform to connect alkyl C-partners with various nitrogen motifs. Notably, the photoinduced Cu-catalyzed strategy pioneered by Fu, Peters, and others allows *N*-alkylation reactions to proceed efficiently even in an enantioselective manner under mild conditions[39-46]. Inspired by this advancement, we questioned whether the Cu-catalyzed C-N coupling of glycosyl radical and *N*-nucleophiles could enable a new manifold for *N*-glycosylation (**Figure 1c**). Herein, we report the development of the first glycosyl radical-mediated *N*-glycosylation reaction using readily accessible, bench-stable glycosyl sulfone donors and unmodified *N*-nucleophiles under mild copper-catalyzed photoredox-promoted conditions (**Figure 1d**). Notably, the new desulfonylative cross-coupling protocol enables facile access to complex *N*-glycosides and nucleosides with unique chemoselectivity profiles.

Reaction discovery: The previous studies have laid out the basic blueprint for photoinduced Cu-catalyzed *N*-alkylation of nitrogen (R_1R_2NH) nucleophiles with alkyl halides[43]. The common reaction manifold for this class of transformations involves the SET activation of an alkyl electrophile by the photoexcited amido-Cu(I) species Cu(I)-N, forming an alkyl radical and a Cu(II)-N intermediate. Subsequently, the alkyl radical reacts with Cu(II)-N to give the *N*-alkylation product and reconstitute Cu(I)[37]. In principle, this manifold could be applied to the reaction of glycosyl halide donors as a specialized set of secondary alkyl halides [47]. In this scenario, a glycosyl radical could be generated from a halide donor and then react with Cu(II)-N to form a Cu(III) intermediate, which affords the *N*-glycosylation product upon reductive elimination (**Figure 1C**). The glycosyl radical could also react with Cu(II) via an outer-sphere mechanism[37] to give the *N*-glycosylation product. The potential problems with this reaction design include the high reduction potential of the most commonly used glycosyl donors and the relatively weak reducing ability of the Cu(I)-N complex[45, 48]. In addition, the SET reactivity of Cu(I)-N could be greatly influenced by the structure of the N-partners[43, 45]. To better facilitate the initial SET, more readily reducible glycosyl donors could be employed[25]. Additionally, an auxiliary electron shuttle could be

a. Model rection of **6**

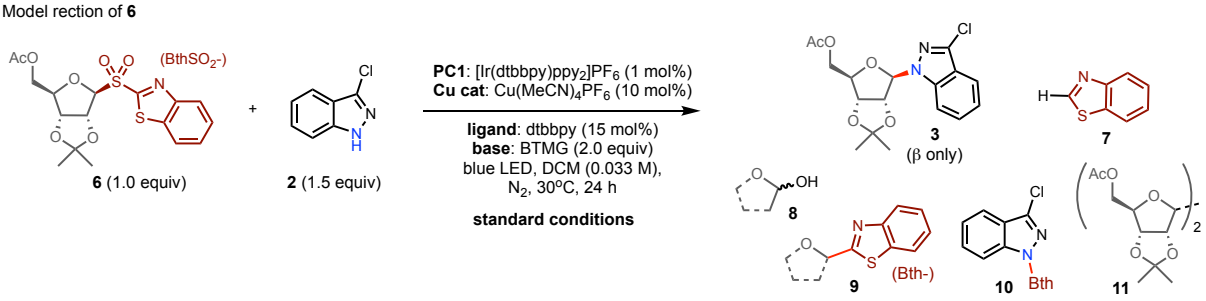

Entry	Variations	yield of **3**[a]	Entry	Variations	yield of **3**[a]	Entry	Variations	yield of **3**[a]
1	no change	88% (85%[b])	9	w/o BTMG base	ND	17	DBU as base	65%
2	20 min	62%	10	w/o dtbbpy ligand	74%	18	K_2CO_3 as base	<5%
3	w/o PC	49%[c]	11	w/ 0.2 mol% **PC1**	85%	19	Et_3N as base	ND
4	w/o PC, 20 min	<3%	12	**PC2** *fac*-Ir(ppy)$_3$[g]	81%	20	green LED (520-525 nm)	64%
5	w/o PC, UV[d]	62%	13	**PC3** [Ir(dtbbpy)(dFppy)$_2$]PF$_6$[g]	40%	21	MeCN as solvent	<5%
6	w/o Cu	6%[e]	14	**PC4** [Ir(dF(CF$_3$)ppy)$_2$dtbbpy]PF$_6$[g]	22%	22	DCM/H_2O (1:1) as solvents	83%
7	w/o light	ND	15	**PC5** Ru(bpy)$_3$Cl$_2$[g]	<5%	23	under air atmosphere	58%
8	w/o PC and Cu	5%[f]	16	**PC6** eosin Y[g]	36%	24	+ TEMPO (2.0 equiv)[h]	ND

b. Reduction potential for selected glycosyl donors and PCs[i]

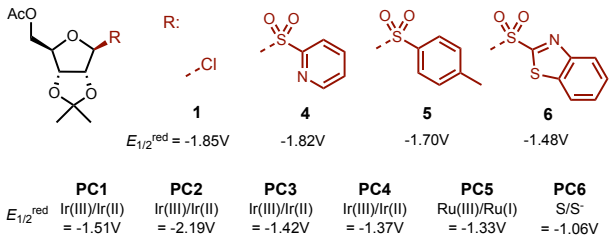

c. Comparison of reaction rates

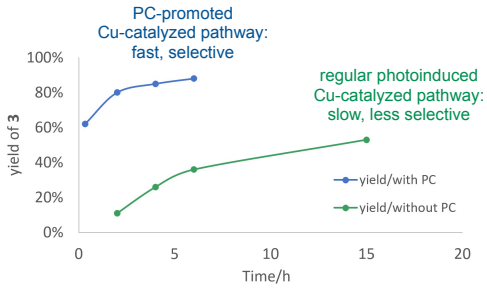

d. Proposed mechanism

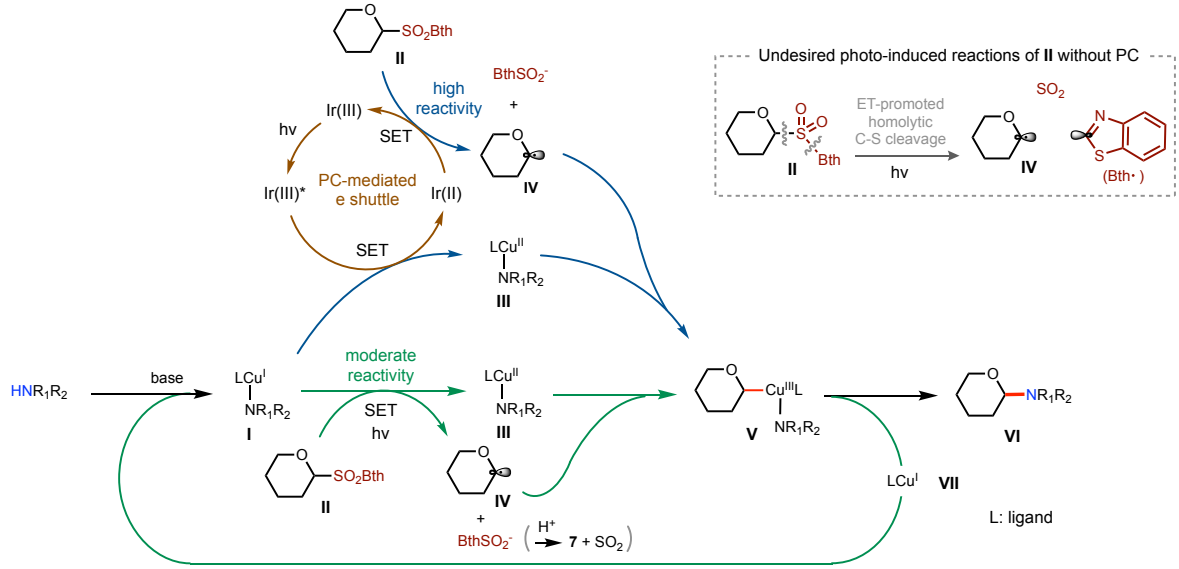

Figure 2. The model *N*-glycosylation reaction of 2 under Cu-catalyzed photoredox-promoted conditions. Standard conditions: **6** (1.0 equiv), **2** (1.5 equiv), [Ir(dtbpy)ppy$_2$]PF$_6$ (1 mol%), Cu(MeCN)$_4$PF$_6$ (10 mol%), dtbbpy (15 mol%), BTMG (2.0 equiv), DCM (0.033 M), N_2, 30 °C, blue LED (465 nm, 48 W), 24 h. [a] Yields were determined by ^{1}H NMR analysis of crude reaction mixtures, using 1,1,2,2-tetrachloroethane as an internal standard. [b] Isolated yield. [c] About 10% of **9** and 26% of **10** were observed. [d] 390nm UV lamp (40 W) was used. [e] About 8% of **9** was observed and the reaction mixture was intractable. [f] The reaction mixture was intractable. [g] **PC1** was replaced with other photocatalysts. [h] TEMPO-adduct product **S-3a** was isolated in 81% yield (See Supplementary Figure S8). [i] Reduction potentials were measured against SCE in CH_3CN. ND: not detected.

introduced to promote the SET between Cu(I)-N and the glycosyl donor[37]. In principle, a photocatalyst (PC) with adequately strong reducing ability could accept an electron from Cu(I)-N and relay it onto the glycosyl donor, forming the putative glycosyl radical and Cu(II)-N[37]. Regrettably, our initial assessment of the reaction between glycosyl chloride donors such as D-ribofuranosyl chloride **1** ($E_{1/2}$ = -1.85V versus (vs.) saturated calomel electrode (SCE) in CH_3CN) and heteroaromatic *N*-nucleophile 3-chloro-1*H*-indazole **2** only generated the desired *N*-glycoside **3** in trace amounts (<3%) under various photoinduced Cu-catalyzed conditions (**Figure 2**). In order to promote the initial SET activation under mild conditions, we turned our attention to glycosyl sulfone donors. Sulfone donors are bench-stable under ambient conditions and can be readily prepared from the corresponding thioglycoside precursors by oxidation with magnesium monoperoxyphthalate [25, 49]. In a previous study, heteroaryl sulfone donors such as 2-pyridyl sulfone (see **4**) and 2-benzothiazolyl sulfone ($BthSO_2$, see **6**) could be activated by SET via an electron-donor-acceptor complex with Hantzsch ester under photoirradiation to generate glycosyl radicals, which were subsequently trapped by electron-deficient alkenes to give *C*-alkyl glycosides[25]. Such sulfone donors could also undergo desulfonylative cross-coupling, via glycosyl radical species, with different aryl partners to give *C*-aryl glycosides through Fe or Ni catalysis [50]. As shown in **Figure 2a**, the model reaction of D-ribofuranosyl benzothiazolyl sulfone donor **6** (1.0 equiv) with **2** (1.5 equiv) afforded *N*-glycoside **3** in moderate yield (49%) using 10 mol% of $Cu(CH_3CN)_4PF_6$ as the catalyst, 15 mol% of 4,4′-di-*tert*-butyl-2,2′-bipyridine (dtbbpy) as the ligand, and 2.0 equiv of 2-*tert*-butyl-1,1,3,3-tetramethylguanidine (BTMG) as the base under the irradiation of 48 W blue LED (465 nm) and N_2 protection in dichloromethane (DCM) at room temperature (rt, approximately 30 °C) (entry 3). Notably, the reaction was relatively slow and poorly selective, giving rise to a mixture of products. About 34% of **2** remained unconsumed after 24 hours; *C*-glycosylation side product **9** bearing a C_1-benzothiazolyl (Bth) group and *N*-arylation side product **10** were formed in 10% and 26% yield, respectively. C-C dimerized[30] side product **11** was also formed in trace amounts (5%). The same reaction under UV irritation (390 nm, 40 W) gave **3** in slightly higher yield but similarly low selectivity (62%, entry 5). Gratifyingly, the yield of **3** could be greatly improved to 88% (β isomer only) when 1 mol% of photocatalyst $[Ir(dtbbpy)ppy_2]PF_6$ (**PC1**) was added (entry 1, standard conditions). Formation of side products **9** (~2%) and **10** (~4%) was mostly suppressed. A 62% yield of **3** was obtained in just 20 min compared to <3% yield under standalone Cu-catalyzed conditions (entries 2 vs. 4 and **Figure 2c**). Overall, the reaction under the cooperative catalysis of Ir PC and Cu was much faster and more chemoselective than that without the PC under photoinduced Cu catalysis.

Control experiments showed that the choice of sulfone donor, the reducing ability of the photocatalyst, Cu(I) catalyst, BTMG base, and photoirradiation were critical to achieving high efficiency for the *N*-glycosylation. Reduction potential measurements vs. SCE in CH_3CN indicated that the $BthSO_2$ donor **6** ($E_{1/2}^{red}$ = -1.48V) is considerably more reducible than 2-pyridyl sulfone **4** ($E_{1/2}^{red}$ = -1.82V) and phenyl sulfone **5** ($E_{1/2}^{red}$ = -1.70V). Neither **4** nor **5** can react with **2** to give **3** under our standard conditions. The reduction potential of **PC1** ($(E_{1/2}^{red}[Ir^{III}/Ir^{II}]$ = -1.51 V) [51] matches well with sulfone donor **6**. **PC2** *fac*-$Ir(ppy)_3$ ($E_{1/2}^{red}[Ir^{III}/Ir^{II}]$ = -2.19 V)[52] is slightly less effective but also worked well (entry 12). The addition of photocatalysts like $[Ir(dtbbpy)(dFppy)_2]PF_6$ (**PC3**), $[Ir(dF(CF_3)ppy)_2$ dtbbpy$]PF_6$ (**PC4**), $Ru(bpy)_3Cl_2$ (**PC5**), or eosin Y (**PC6**) gave lower yields of **3** than the standalone Cu catalysis (entries 13-16 vs. 3). The combination of **PC2** and chloride donor **1** did not furnish any product **3** under various

conditions, indicating the importance of a delicate interplay between the Cu-mediated and photocatalyst-mediated pathways. No conversion of **6** took place in the absence of LED irradiation (entry 7). Irradiation with green LED gave a slightly lower yield of **3** than blue LED (entry 20). A sufficiently strong base was necessary for high efficiency. Both BTMG (p*K*a = 23.6 in MeCN)[53] and 1,8-diazabicyclo(5.4.0)undec-7-ene (DBU, p*K*a = 24.3 in MeCN)[53] could promote this reaction, but DBU exhibited lower reactivity (entry 17). Product **3** was formed in <5% yield when Et_3N or K_2CO_3 was used as the base (entries 18, 19). Other Cu catalysts could also work but were not as effective as $Cu(MeCN)_4PF_6$ (See Supplementary Table S4). The use of dtbbpy ligand boosted the yield but was not essential (entries 10 vs. 1 and Supplementary Table S6). The reaction worked best in halogenated hydrocarbon solvents. CH_3CN and THF provided little amounts of the desired product (entry 21 and Supplementary Table S2 & S5). The performance of the reaction diminished under air atmosphere (entry 23). Interestingly, water was well-tolerated, and the reaction in the biphasic medium of DCM and H_2O (v/v = 1:1) gave similar results (~83% yield of **3**, entry 22). Trace amounts of side product **8** were formed under most of the conditions tested.

The addition of 2.0 equiv of 2,2,6,6-tetramethylpiperidinooxy (TEMPO) to the reaction of **2** and **6** under the same optimized conditions inhibited the formation of **3** and delivered the *O*-glycosylation product **S-3a** bearing an *O*-linked TEMPO moiety in high yield (See Supplementary Figure S8)[31]. This observation suggests that a glycosyl radical intermediate is likely generated under the reaction conditions, and the coupling of glycosyl radical with TEMPO is faster than the Cu-catalyzed C-N coupling. Control experiments further showed that sulfone donor **6** alone was stable under LED irradiation, but underwent homolytic C-S bond cleavage in the reaction mixture to generate both glycosyl radical and benzothizolyl radical Bth• in the absence of the photocatalyst and Cu catalyst (entry 8). We suspected that a photoinduced energy transfer (ET) between **6** and the conjugate base of **2** could promote the homolytic C-S cleavage of **6**, leading to the formation of significant amounts of side products **9**, **10**, and **11** under the regular photoinduced Cu-catalyzed *N*-glycosylation conditions (**Figure 1d**). Stern-Volmer quenching experiments showed that $Cu(MeCN)_4PF_6$, glycosyl sulfone **6**, 3-chloroindazole **2** alone or the mixture of $Cu(MeCN)_4PF_6$ and **2** did not quench the fluorescence of Ir **PC1**. Notably, the mixture of $Cu(MeCN)_4PF_6$, **2**, and BTMG base quenched the luminescence of **PC1** in the excited state, suggesting that the amido complex of Cu(I) and **2** interact with the photocatalyst under photoirradiation (See Supplementary Figure S11-S16 for details).

Based on the above evidence and previous reports, the following reaction pathways were proposed for this photoredox/Cu-catalyzed *N*-glycosylation of indazole (R_1R_2NH) with benzothiazolyl sulfone donor **II** (**Figure 1d**): (1) Cu(I) complex alone can catalyze the radical-mediated C-N coupling under LED irradiation, providing a regular reaction pathway for the *N*-glycosylation (shown in green arrows). R_1R_2NH first forms an amido-Cu(I) complex **I** with the assistance of BTMG base. The SET between photoexcited Cu(I)-N **I** and sulfone donor **II** gives glycosyl radical intermediate **IV** and Cu(II)-N complex **III**. The resulting $BthSO_2$- can fragment to **7** and SO_2 upon protonation. **IV** can react with **III** to give *N*-glycosylation product **VI** via either Cu(III) intermediate **V** or an outer-sphere mechanism and reconstitute Cu(I) [37]. This pathway is viable but proceeds with low efficiency and product selectivity. The weak SET-reducing ability of **I** under photoirradiation is probably the main cause of the observed low reactivity. On the other hand, sulfone **II** could also slowly undergo homolytic C-S cleavage to give **IV**, Bth• and SO_2 through photoinduced ET[54, 55]. Such competitive homolytic C-S cleavage could induce undesired side reactions. (2) Photocatalysts such as Ir(III) **PC1** under LED irradiation can alter the electron flow between

Cu(I)-N **I** and sulfone donor **II**, providing a faster and more chemoselective pathway for the *N*-glycosylation (shown in blue arrows). The photoexcited Ir(III) can readily accept an electron from Cu(I)-N to generate Ir(II) and Cu(II)-N **III**. Ir(II) with a high reduction potential can donate an electron to sulfone donor **II** to return to its original Ir(III) state, furnishing glycosyl radical **IV**. **IV** and **III** then react to give **VI** and reconstitute Cu(I). The observed stereochemical outcome of **VI** could be rationalized by the stabilizing orbital interaction between the ring oxygen and the newly formed C_1-Cu bond in the transition state[56]. The resulting **V** is possibly also stabilized by the metallo-anomeric effect[56] (donation of electron density from the ring oxygen into the C_1-Cu σ* antibonding orbital). Inner-sphere stereoretentive reductive elimination then furnishes **VI** in high stereoselectivity. Overall, the photocatalyst serves as an electron shuttle between Cu(I)-N and the sulfone donor, providing a more efficient track for the Cu-catalyzed *N*-glycosylation reaction[41]. Due to the rate acceleration of the desired *N*-glycosylation, the impact of ET-induced homolytic C-S cleavage is alleviated.

Substrate scope: The optimized *N*-glycosylation reaction conditions were then applied to the cross-coupling of a range of *N*-nucleophiles with D-ribofuranosyl donor **6** (**Figure 3**). As demonstrated in the previous disclosures of photoinduced Cu-catalyzed *N*-alkylation[40, 42, 43], *N*-nucleophiles in which nitrogen was either part of an aromatic ring or attached to an arene generally worked well in this system. *N*-heteroarenes with relatively acidic NH groups[57, 58] (p*K*a < 20) typically showed high reactivity and proceeded with high β stereoselectivity. Acidic NH groups presumably allowed the facile formation of the requisite amido-Cu(I) complex. For example, 1*H*-indazoles bearing various substituents including chloride (**3**), bromide (**16**), iodide (**13**), fluoride (**18**), ester (**15**), ether (**17**), and aldehyde (**14**) afforded the desired *N*-glycosides in good to high yields and with exclusive β selectivity. Triazole (**19**, **20**), azaindole (**21**, **22**), and pyrrole (**25**) also served as effective substrates. The reactions of carbazole and 1,2,3-benzotriazole gave the corresponding *N*-glycosides **36** and **20** in good yields and with slightly eroded stereoselectivity (β/α = 7.5:1, >10:1). Interestingly, the reaction of methyl 1*H*-1,2,4-triazole-3-carboxylate, a precursor of antiviral drug ribavirin, with **6** furnished N_2-glycosylated product **19** in excellent yield, whereas its *N*-glycosylation via the typical ionic pathway selectively occurred at the N_1 position. We speculated that the ester group might act as a directing group to facilitate the N_2-selective Cu(I)-N complexation and the subsequent C-N coupling. Cross-coupling with indoles with less acidic NH groups (p*K*a = 21) also proceeded with high yield but lower stereoselectivity. For example, *N*-glycosylation of the indole side chain of *N*-Boc tryptophan methyl ester generated product **24** as a mixture of anomers (β/α = 1.8:1) in excellent yield**.** Notably, various purine derivatives underwent reactions to secure the corresponding *N*-nucleoside analogs in moderate to good yields (46%-84%) and with exclusive β selectivity. Glycosylation with plain purine gave product **26** as a mixture of N_9/N_7 (1.3:1) regioisomers, whereas the reaction of C_6-substituted purine (e.g. **27**) proceeded with significantly enhanced N_9 site selectivity. N_6-bis(*tert*-butoxycarbonyl) adenine, N_6-benzyladenine, and N_2-isobutyryl guanine (**28**-**30**) selectively reacted at the N_9 position. Cross-coupling of O_6-benzyl protected guanine bearing an unprotected heteroaryl C_2-NH_2 group afforded the N_9-glycosylated product **31** in high regio- and stereoselectivity. The O-protecting group of purines not only influenced the N_7/N_9 regioselectivity but also improved the solubility (**31**). In contrast to purines, the reactions of pyrimidine nucleoside bases in various protected forms did not give the desired *N*-glycosylation products (e.g. **32**) in useful yields (<5%) under the optimized conditions. We reasoned that the neighboring carbonyl group of N_1H might hamper the Cu(I)-N complexation and/or the subsequent C-N coupling step.

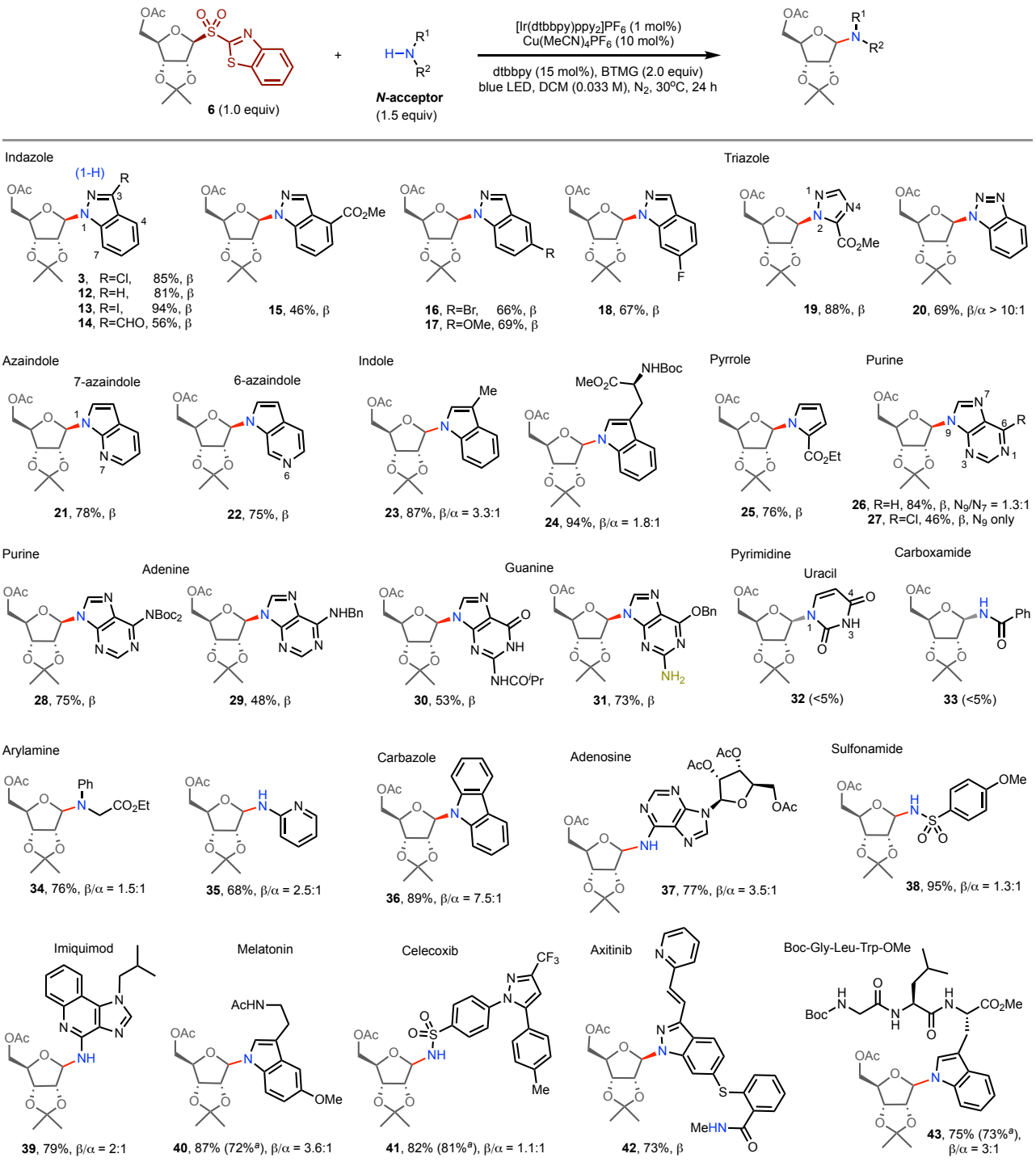

Figure 3. Scope of *N*-nucleophiles in the Cu-catalyzed *N*-glycosylation reactions with sulfone donor 6. Standard conditions: **6** (1.0 equiv), ***N*-acceptor** (1.5 equiv), **PC1** (1 mol%), Cu cat (10 mol%), ligand (15 mol%), base (2.0 equiv), DCM (0.033 M), N_2, 30 °C, blue LED (465 nm, 48 W), 24 h. Isolated yield at a 0.1 mmol scale. The ratio of α/β isomers was determined by ^{1}H NMR or chromatographic analysis of the reaction mixture. [a] Conducted in a mixed solvent mixture of DCM/H_2O (v/v = 2:1).

The *N*-glycosylation of arylamines, such as 2-pyridiylamine (**35**) and adenosine (**37,** through C_6-NH_2), typically proceeded with good yields but with low to moderate stereoselectivity. The NH_2 group of

sulfonamides, a common pharmacophore, could also be glycosylated in excellent yield but with low stereoselectivity (see **38,** β/α = 1.3:1). In contrast, the NH groups of alkylamines and carboxamides were considerably less acidic and did not undergo the desired *N*-glycosylation under our optimized conditions (see **33**). The underlying reason for the diminished stereoselectivity detected for certain *N*-nucleophiles is unclear at this stage. We surmised that different mechanisms (inner-sphere or outer-sphere pathways[37]) might be operative during the C-N bond-forming step for different *N*-nucleophiles, which leads to varying stereochemical outcomes.

As shown in **Figure 3**, *N*-glycosylation with sulfone donor **6** can be applied to the late-stage *N*-glycosylation of complex molecules. Imiquimod (a TLR7 agonist for treating carcinoma, **39**) was selectively glycosylated through its pyridylamine group in 79% yield. Indole *N*-glycosylation of the sleep hormone melatonin in the presence of an *N*-acetamide group afforded **40** in 87% yield with moderate stereoselectivity (β/α = 3.6:1). Celecoxib, a selective Cox-2 inhibitor, was glycosylated on the sulfonamide group to give **41** in 82% yield. The indazole moiety of the antitumor drug Axitinib was selectively glycosylated to give product **42** with good yield and excellent β selectivity. The reaction of tripeptide Boc-Gly-Leu-Trp-OMe furnished the corresponding *N*-glycopeptide (**43**) in good yield. Notably, the reactions of **40**, **41**, and **43** in the biphasic medium of DCM and H_2O (v/v = 2:1) gave similar results to the reactions performed in anhydrous DCM.

As shown in **Figure 4**, the desulfonylative *N*-glycosylation method can be applied to the reactions of a variety of benzothioazolyl sulfone glycosyl donors with different N-nucleophiles. Both furanosyl and pyranosyl sulfone donors reacted with 3-chloro-1*H*-indazole **2** to give the corresponding *N*-glycosides in good to excellent yields. Overall, sulfone donors derived from ribose (**44**), 5-deoxy-ribose (**45**), mannofuranose (**51**), arabinofuranose (**49**), rhamnose (**54**), galactose (**56**), and mannose (**57**) exhibited excellent stereoselectivity, while the reactions of glucose (**52**) and xylose (**55**) donors were less stereoselective. The structure of mannofuranose **51** was confirmed by X-ray diffraction, whereas the structures of the other *N*-glycoside products were analyzed by NMR spectra (See Supplementary Figure S22 and NMR spectra for more details). Efforts to improve the reaction's stereochemical outcome by using a neighboring group participation strategy were unsuccessful in our hands. C_2-OAc-protected glycosyl sulfone donors were relatively unstable under our standard reaction conditions. For instance, glycosyl sulfone donor **53** readily underwent elimination to give a C_1-sulfonyl glycal product. As highlighted by compounds **46**-**48**, **50**, and **58**, various purine-based products were obtained in moderate to good yields as single stereoisomers. Protected *N*-Man-Trp **59** was isolated in 64% yield with elusive α stereoselectivity.

Contrary to the high reactivity of hydroxyl groups in oxocarbenium-mediated glycosylation reactions, alkyl OH groups did not participate in *O*-glycosylation under our Cu-catalyzed reaction conditions. The low acidity and poor binding affinity of hydroxyl units with Cu might have precluded the formation of Cu-O(alkyl) species. Similarly, water did not interfere with the Cu-catalyzed radical-mediated pathway. It is worth mentioning that phenolic hydroxyl groups possess sufficient acidity and redox reactivity and can thereby react with glycosyl sulfone donors to give the corresponding phenolic *O*-glycosides in moderate yields under our standard conditions (See Supplementary Figure S21). Taking advantage of the inertness of aliphatic OH groups under our reaction conditions, we employed the catalytic regime to selectively glycosylate the reactive NH sites of complex substrates bearing unprotected alcohols. For example, carvedilol, a hypertension drug, was exclusively *N*-glycosylated on the carbazole nitrogen in moderate

yield without affecting the secondary alkyl amine and alkyl hydroxyl group (**60**). *C*-glycosyl benzothiazole **9** and glycosyl dimer **11** were also detected as byproducts. The nucleoside core of antivirus drug remdesivir and adenosine reacted with mannosyl or arabinosyl sulfone donors to give the corresponding *N*-glycosides **61** and **62**, respectively in moderate yields and excellent chemoselectivity.

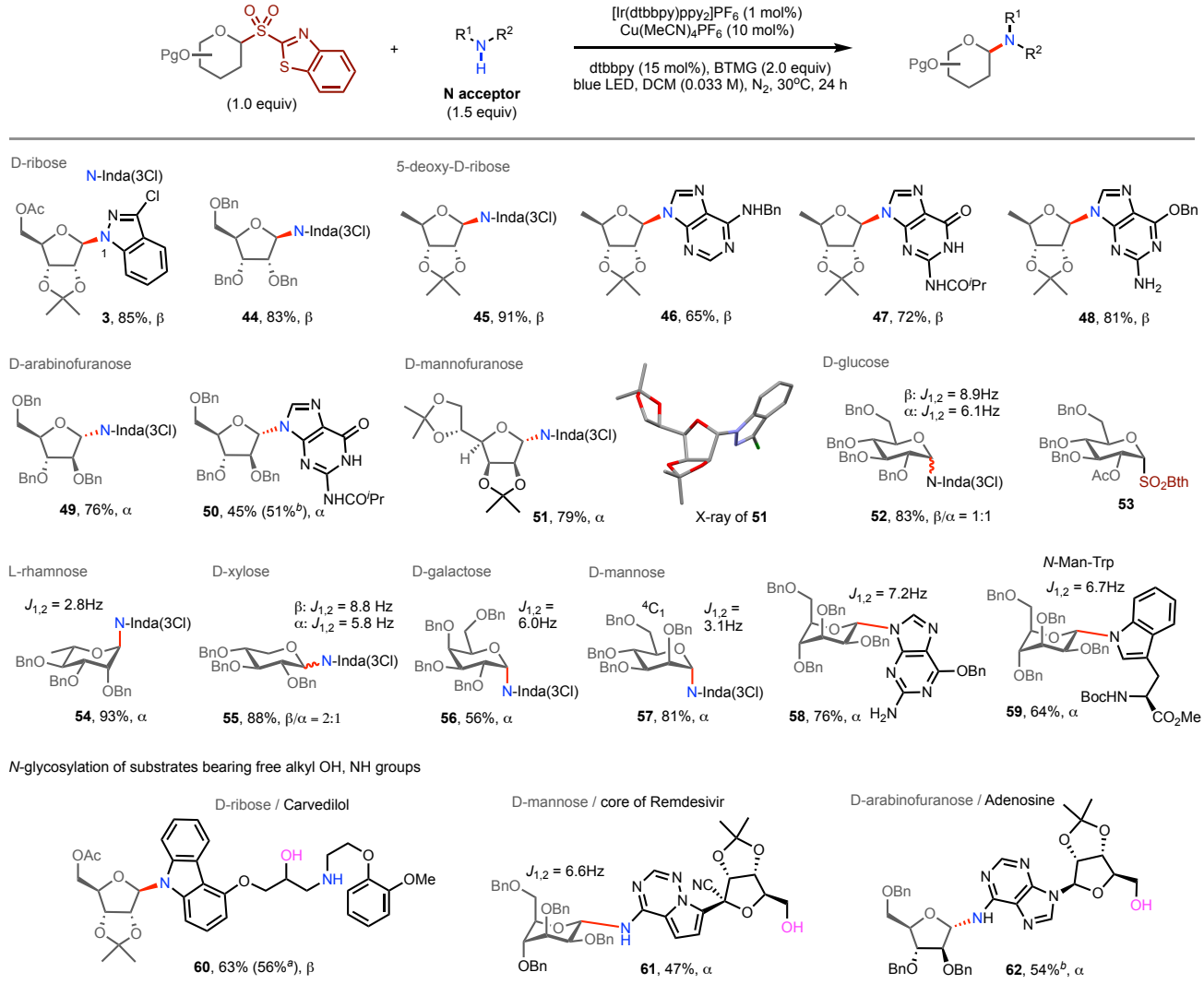

Figure 4. **Substrate scope of the Cu-catalyzed desulfonylative *N*-glycosylation reaction.** Isolated yield at a 0.1 mmol scale. The ratios of α/β isomers were determined by ^{1}H NMR or chromatographic analysis of the reaction mixture. [a] Conducted in a mixed solvent mixture of DCM/H_2O (v/v = 2:1). [b] 1.0 equiv of *N*-acceptor and 1.5 equiv of glycosyl sulfone were used.

In summary, we have developed an unprecedented glycosyl radical-mediated *N*-glycosylation reaction under copper/photoredox dual catalysis. The identification of readily reducible benzothiazolyl sulfones as glycosyl donors was the key to achieving radical *N*-glycosylation reactivity with *N*-nucleophiles under regular photoinduced Cu-catalyzed conditions. The addition of an appropriate photocatalyst provided an electron shuttle to facilitate more efficient SET activation of the sulfone donor, which significantly accelerated the *N*-glycosylation process. The catalytic method was successfully applied to prepare a variety of complex *N*-glycosides such as nucleosides and their analogs from easily accessible precursors. Of particular note, this radical *N*-glycosylation protocol exhibits high chemoselectivity and water tolerance, effectively overcoming the inherent problems associated with traditional cationic glycosylations.

We expect this work to further encourage the development of glycosyl radical-mediated cross-coupling reactions with other heteroatomic reagents to assemble a broader array of medicinally valuable carbohydrates that are otherwise difficult to access by other means.

Methods:

A typical procedure for copper/photoredox catalysed desulfonylative radical *N*-glycosylation: An 8 mL vial equipped with a magnetic stir bar was charged with glycosyl sulfone **6** (41.3 mg, 0.1 mmol, 1.0 equiv), **2** (22.8 mg, 0.15 mmol, 1.5 equiv), $[Ir(dtbbpy)ppy_2]PF_6$ (0.9 mg, 0.001 mmol, 1 mol%), $Cu(MeCN)_4PF_6$ (3.7 mg, 0.01 mmol, 10 mol%), dtbbpy (4.0 mg, 0.015 mmol, 15 mol%), anhydrous DCM (3.0 mL), and BTMG (34.2 mg, 0.2 mmol, 2.0 equiv). The reaction vial was then purged with N_2 and sealed with a PTFE cap. The reaction mixture was allowed to stir vigorously under blue LED irradiation at approximately 30 °C for 24 h before being concentrated under reduced pressure. The resulting residue was purified by silica gel column chromatography to give product **3** as a colorless oil in 85% yield (R_f = 0.6, Hexane:EtOAc = 5:1).

References:

1. Shivatare, S. S., Shivatare, V. S. & Wong, C.-H. Glycoconjugates: Synthesis, Functional Studies, and Therapeutic Developments. *Chem. Rev.* **122**, 15603-15671 (2022).
2. Yang, Y., Zhang, X. & Yu, B. *O*-Glycosylation methods in the total synthesis of complex natural glycosides. *Nat. Prod. Rep.* **32**, 1331-1355 (2015).
3. Bokor, É. et al. *C*-Glycopyranosyl Arenes and Hetarenes: Synthetic Methods and Bioactivity Focused on Antidiabetic Potential. *Chem. Rev.* **117**, 1687-1764 (2017).
4. Hsu, C.-H., Hung, S.-C., Wu, C.-Y. & Wong, C.-H. Toward automated oligosaccharide synthesis. *Angew. Chem. Int. Ed.* **50**, 11872-11923 (2011).
5. Sangwan, R., Khanam, A. & Mandal, P. K. An Overview on the Chemical N-Functionalization of Sugars and Formation of N-Glycosides. *Eur. J. Org. Chem.* **2020**, 5949-5977 (2020).
6. Jordheim, L. P., Durantel, D., Zoulim, F. & Dumontet, C. Advances in the development of nucleoside and nucleotide analogues for cancer and viral diseases. *Nat. Rev. Drug. Discov.* **12**, 447-464 (2013).
7. Zhang, Q., Sun, J., Zhu, Y., Zhang, F. & Yu, B. An Efficient Approach to the Synthesis of Nucleosides: Gold(I)-Catalyzed N-Glycosylation of Pyrimidines and Purines with Glycosyl ortho-Alkynyl Benzoates. *Angew. Chem. Int. Ed*. **50**, 4933-4936 (2011).
8. Stanley P., et al. N-Glycans. in Varki A. et al. editors. *Essentials of Glycobiology [Internet] 4th edition* (Cold Spring Harbor (NY) Cold Spring Harbor Laboratory Press; 2022. Chapter 9).
9. Chen, Z., Sato, S., Geng, Y., Zhang, J. & Liu, H.-W. Identification of the Early Steps in Herbicidin Biosynthesis Reveals an Atypical Mechanism of C-Glycosylation. *J. Am. Chem. Soc.* **144**, 15653-15661 (2022).
10. Loustaud-Ratti, V. et al. Ribavirin: Past, present and future. *World J Hepatol* **8**, 123-130 (2016).
11. Staudacher, E., Van Damme, E. J. M. & Smagghe, G. Glycosylation-The Most Diverse Post-Translational Modification. *Biomolecules* **12**, 1313 (2022).
12. Chakraborty, S., Mishra, B., Das, P. R., Pasari, S. & Hotha, S. Synthesis of *N*-Glycosides by Silver-Assisted Gold Catalysis. *Angew. Chem. Int. Ed.* **62**, e202214167 (2023).
13. Ding, F., William, R. & Liu, X.-W. Ferrier-Type *N*-Glycosylation: Synthesis of *N*-Glycosides of Enone Sugars. *J. Org. Chem.* **78**, 1293-1299 (2013).
14. Li, P. et al. Glycosyl *ortho*-(1-phenylvinyl)benzoates versatile glycosyl donors for highly efficient synthesis of both *O*-glycosides and nucleosides. *Nat. Commun.* **11**, 405 (2020).

15. Liu, R. et al. Synthesis of Nucleosides and Deoxynucleosides via Gold(I)-Catalyzed *N*-Glycosylation of Glycosyl (*Z*)-Ynenoates. *Org. Lett.* **24**, 9479-9484 (2022).
16. Nielsen, M. M. & Pedersen, C. M. Catalytic Glycosylations in Oligosaccharide Synthesis. *Chem. Rev.* **118**, 8285-8358 (2018).
17. Panza, M., Pistorio, S. G., Stine, K. J. & Demchenko, A. V. Automated Chemical Oligosaccharide Synthesis: Novel Approach to Traditional Challenges. *Chem. Rev.* **118**, 8105-8150 (2018).
18. Kobayashi, Y., Nakatsuji, Y., Li, S., Tsuzuki, S. & Takemoto, T. Direct *N*-Glycofunctionalization of Amides with Glycosyl Trichloroacetimidate by Thiourea/Halogen Bond Donor Co-Catalysis. *Angew. Chem. Int. Ed*. **57**, 3646-3650 (2018).
19. An, S. et al. Palladium-Catalyzed *O*- and *N*-Glycosylation with Glycosyl Chlorides. *CCS Chem.* **3**, 1821-1829 (2021).
20. Toshima, K. & Tasuta, K. Recent progress in *O*-glycosylation methods and its application to natural products synthesis. *Chem. Rev.* **93**, 1503-1531 (1993)
21. Mukherjee, M. M., Ghosh, R. & Hanover, J. A. Recent Advances in Stereoselective Chemical *O*-Glycosylation Reactions. *Front. Mol. Biosci.* **9**, 896187 (2022).
22. Chen, A. et al. Recent advances in glycosylation involving novel anomeric radical precursors. *J. Carbohydr. Chem.* **40**, 361-400 (2021).
23. Xu, L.-Y., Fan, N.-L. & Hu, X.-G. Recent development in the synthesis of *C*-glycosides involving glycosyl radicals. *Org. Biomol. Chem.* **18**, 5095-5109 (2020).
24. Jiang, Y., Zhang Y., Lee, B. C. & Koh, M. J. Diversification of Glycosyl Compounds via Glycosyl Radicals. *Angew. Chem. Int. Ed.* **62**, e202305138 (2023).
25. Wang, Q. et al. Visible light activation enables desulfonylative cross-coupling of glycosyl sulfones. *Nat. Synth.* **1**, 967-974 (2022).
26. Jiang, Y., Wang, Q., Zhang, X. & Koh, M. J. Synthesis of C-glycosides by Ti-catalyzed stereoselective glycosyl radical functionalization. *Chem* **7**, 3377-3392 (2021).
27. Xu, S. et al. Generation and Use of Glycosyl Radicals under Acidic Conditions: Glycosyl Sulfinates as Precursors. *Angew. Chem. Int. Ed.* **62**, e202218303 (2023).
28. Shang, W. et al. Generation of Glycosyl Radicals from Glycosyl Sulfoxides and Its Use in the Synthesis of *C*-linked Glycoconjugates. *Angew. Chem. Int. Ed.* **60**, 385-390 (2021).
29. Nagatomo, M. & Inoue, M. Convergent Assembly of Highly Oxygenated Natural Products Enabled by Intermolecular Radical Reactions. *Acc. Chem. Res.* **54**, 595-604 (2021).
30. Masuda, K., Nagatomo, M. & Inoue, M. Direct assembly of multiply oxygenated carbon chains by decarbonylative radical–radical coupling reactions. *Nat. Chem.* **9**, 207-212 (2017).
31. Wang, Q. et al. Iron-catalysed reductive cross-coupling of glycosyl radicals for the stereoselective synthesis of C-glycosides. *Nat. Synth.* **1**, 235-244 (2022).
32. Wei, Y., Ben-zvi, B. & Diao, T. Diastereoselective Synthesis of Aryl *C*-Glycosides from Glycosyl Esters via C−O Bond Homolysis. *Angew. Chem. Int. Ed.* **60**, 9433-9438 (2021).
33. Zhu, F. et al. Catalytic and Photochemical Strategies to Stabilized Radicals Based on Anomeric Nucleophiles. *J. Am. Chem. Soc.* **142**, 11102-11113 (2020).
34. Liu, J. & Gong, H. Stereoselective Preparation of α-*C*-Vinyl/Aryl Glycosides via Nickel-Catalyzed Reductive Coupling of Glycosyl Halides with Vinyl and Aryl Halides. *Org. Lett.* **20**, 7991-7995 (2018).
35. Zhang, C. et al. Halogen-bond-assisted radical activation of glycosyl donors enables mild and stereoconvergent 1,2-*cis*-glycosylation. *Nat. Chem.* **14**, 686-694 (2022).
36. Zuo, H., Zhang, C., Zhang, Y. & Niu, D. Base-Promoted Glycosylation Allows Protecting Group-Free and Stereoselective *O*-Glycosylation of Carboxylic Acids. *Angew. Chem. Int. Ed.* **62**, e202309887 (2023).
37. Hossain, A., Bhattacharyya, A., & Reiser, O. Copper's rapid ascent in visible-light photoredox catalysis. *Science* **364**, eaav9713 (2019).

38. Alvarez, E. M. et al. *O*-, *N*- and *C*-bicyclopentylation using thianthrenium reagents. *Nat. Synth.* **2**, 548-556 (2023).
39. Chen, J. J. et al. Enantioconvergent Cu-catalysed *N*-alkylation of aliphatic amines. *Nature* **618**, 294-300 (2023).
40. Bissember, A. C., Lundgren, R. J., Creutz, S. E., Peters, J. C. & Fu, G. C. Transition-Metal-Catalyzed Alkylations of Amines with Alkyl Halides: Photoinduced, Copper-Catalyzed Couplings of Carbazoles. *Angew. Chem. Int. Ed.* **52**, 5129-5133 (2013).
41. Liang, Y., Zhang, X. & MacMillan, D. W. C. Decarboxylative sp^3 C-N coupling via dual copper and photoredox catalysis. *Nature* **559**, 83-88 (2018).
42. Creutz, S. E., Lotito, K. J., Fu, G. C. & Peters, J. C. Photoinduced Ullmann C–N Coupling: Demonstrating the Viability of a Radical Pathway. *Science* **338**, 647-651 (2012)
43. Kainz, Q. M. et al. Asymmetric copper-catalyzed C-N cross-couplings induced by visible light. *Science* **351**, 681-684 (2016).
44. Caiger, L., Zhao, H., Constantin, T., Douglas, J. J. & Leonori, D. The Merger of Aryl Radical-Mediated Halogen-Atom Transfer (XAT) and Copper Catalysis for the Modular Cross-Coupling-Type Functionalization of Alkyl Iodides. *ACS Catal.* **13**, 4985-4991 (2023).
45. Dong, X.-Y., Li, Z.-L., Gu, Q.-S. & Liu, X.-Y. Ligand Development for Copper-Catalyzed Enantioconvergent Radical Cross-Coupling of Racemic Alkyl Halides. *J. Am. Chem. Soc*. **144**, 17319-17329 (2022).
46. Górski, B., Barthelemy, A.-L., Douglas, J. J., Juliá, F. & Leonori, D. Copper-catalysed amination of alkyl iodides enabled by halogen-atom transfer. *Nat. Catal.* **4**, 623-630 (2021).
47. Singh, Y., Geringer, S. A. & Demchenko, A. V. Synthesis and Glycosidation of Anomeric Halides: Evolution from Early Studies to Modern Methods of the 21st Century. *Chem. Rev.* **122**, 11701-11758 (2022).
48. Le, C., Chen, T. Q., Liang, T., Zhang, P. & Macmillan, D. W. C. A radical approach to the copper oxidative addition problem: Trifluoromethylation of bromoarenes. *Science* **360**, 1010-1014 (2018).
49. Oka, N., Mori, A., Suzuki, K. & Ando, K. Stereoselective Synthesis of Ribofuranoid *exo*-Glycals by One-Pot Julia Olefination Using Ribofuranosyl Sulfones. *J. Org. Chem*. **86**, 657-673 (2021).
50. Wang, Q., Lee, B. C., Song, N. & Koh, M. J. Stereoselective *C*-Aryl Glycosylation by Catalytic Cross-Coupling of Heteroaryl Glycosyl Sulfones. *Angew. Chem. Int. Ed*. **62**, e202301081 (2023).
51. Lowry, M. S. et al. Single-Layer Electroluminescent Devices and Photoinduced Hydrogen Production from an Ionic Iridium(III) Complex. *Chem. Mater.* **17**, 5712-5719 (2005).
52. Prier, C. K., Rankic, D. A. & MacMillan, D. W. C. Visible Light Photoredox Catalysis with Transition Metal Complexes: Applications in Organic Synthesis. *Chem. Rev*. 2013. **113**, 5322-5363 (2013).
53. Lemaire, C. F. et al. Fast Production of Highly Reactive No-Carrier-Added [^{18}F]Fluoride for the Labeling of Radiopharmaceuticals. *Angew. Chem. Int. Ed.* **49**, 3161-3164 (2010).
54. Nambo, M., Maekawa, Y. & Crudden, C. M. Desulfonylative Transformations of Sulfones by Transition-Metal Catalysis, Photocatalysis, and Organocatalysis. *ACS Catal.* **12**, 3013-3032 (2022).
55. Corpas, J., Kim-Lee, S.-H., Mauleón, P., Arrayás, R. G. & Carretero, J. C. Beyond classical sulfone chemistry: metal- and photocatalytic approaches for C–S bond functionalization of sulfones. *Chem. Soc. Rev.* **51**, 6774-6823 (2022).
56. Zhu, F. & Walczak, M. A. Stereochemistry of Transition Metal Complexes Controlled by the Metallo-Anomeric Effect. *J. Am. Chem. Soc.* **142**, 15127-15136 (2020).
57. Bordwell, F. G. Equilibrium acidities in dimethyl sulfoxide solution. *Acc. Chem. Res.* **21**, 456-463 (1988).
58. Lõkov, M. et al. On the Basicity of Conjugated Nitrogen Heterocycles in Different Media. *Eur. J. Org. Chem.* **2017**, 4475-4489 (2017).

Supplementary information: Detailed synthetic procedures, additional control experiments, compound characterization, LC-MS trace, X-ray crystallography, and NMR spectra.

Data and materials availability: All data are available in the main text or the supplementary materials.

Acknowledgments: This work was supported by the National Key R&D Program of China: 2022YFA1504303, the National Natural Science Foundation of China: 92256302, Frontiers Science Center for New Organic Matter: 63181206, Fundamental Research Funds for the Central Universities: NKU63231195, Haihe Laboratory of Sustainable Chemical Transformations (G.C.), and the Ministry of Education of Singapore Academic Research Fund Tier 2: A-8000941-00-00 (M.J.K.).

Author contributions: Q.S. and Q.W. contributed equally to this work. Q.K. was responsible for the initial discovery of Cu-catalyzed *N*-glycosylation reaction and conducted most of the substrate scope exploration and mechanistic studies, Q. W. was heavily involved in the reaction optimization and mechanistic studies. W.Q. helped with expanding the substrate scope. K.J. conducted the reduction potential measurement experiments. G.H. supervised parts of the project. M.J.K. supervised the project and edited the manuscript. G.C. oversaw the entire project and wrote the manuscript.

Competing interests:
The authors declare no competing financial interests.